

# Nonlinear coherent heat machines and closed-system thermodynamics

Tomáš Opatrný,<sup>1</sup> Šimon Bräuer,<sup>1</sup> Abraham G. Kofman,<sup>2,3</sup> Avijit Misra,<sup>2,3</sup>  
Nilakantha Meher,<sup>2,3</sup> Ofer Firstenberg,<sup>4</sup> Eilon Poem,<sup>4</sup> and Gershon Kurizki<sup>3</sup>

<sup>1</sup>*Department of Optics, Faculty of Science, Palacký University,  
17. listopadu 50, 77146 Olomouc, Czech Republic*

<sup>2</sup>*International Center of Quantum Artificial Intelligence for Science and Technology  
(QuArtist) and Department of Physics, Shanghai University, 200444 Shanghai, China*

<sup>3</sup>*Department of Chemical and Biological Physics,  
Weizmann Institute of Science, Rehovot 7610001, Israel*

<sup>4</sup>*Physics of Complex Systems, Weizmann Institute of Science, Rehovot 7610001, Israel*  
(Dated: August 2, 2022)

All existing heat machines are dissipative open systems. Hence, they cannot operate fully coherently. We propose to replace this conventional thermodynamic paradigm by a completely different one, whereby heat machines are nonlinear coherent closed systems comprised of few field modes. Their thermal-state input is transformed by nonlinear interactions into non-thermal output with controlled quantum fluctuations and the capacity to deliver work in a chosen mode. This new paradigm allows the bridging of quantum coherent and thermodynamic descriptions.

## I. INTRODUCTION

A heat engine may be viewed as a device capable of two functionalities. First, it *must concentrate the energy* of a heat bath in a selected degree of freedom called the working mode, within limits dictated by the first and second laws of thermodynamics. The enormous number of bath modes characteristic of existing heat engines (HE) justifies the thermodynamic paradigm, dating back to Carnot, that describes HE as *open systems dissipated by thermal baths* [1–6]. Second, the concentrated *heat must be partly converted into work output*, which requires the state of the working mode (piston), be it classical or quantum mechanical [3–31] to be *non-passive*, i.e. store ergotropy [14–16, 32–34]. The required non-passivity/ergotropy is achievable either via external control of the piston in HE [5–23] or via information readout and feedforward by an observer (Maxwell’s Demon) in information engines [35–39]. Other means of producing ergotropy/ non-passivity in HE fed by bosonic thermal fields have not been explored thus far.

These long-standing principles have not been revised by recent trends to incorporate quantum information methodology into thermodynamics, known as the resource theory of quantum thermodynamics [40–44]. These trends have mainly focused on *linear Gaussian operations* (LIGO) jointly performed on quantum systems and their thermal bath ancillae. The realization and possible implications of unitary *non-Gaussian operations* (NGO), which have been conceived in quantum optical and quantum information schemes [45–49], are mostly uncharted terrain in the context of HE (but cf. [19]).

Here we break away from the established open-system thermodynamic description and introduce a new paradigm whereby a HE can be a *purely coherent, energy-preserving (autonomous) closed system*. This paradigm is based on *nonlinear coupling of thermal bosonic field*

*modes*, which makes such devices fundamentally different from existing HE that are energized by baths comprised of *linearly coupled modes* [1–31, 39, 50–59]. These devices, dubbed here *heat engines via nonlinear interference* (HENLI), are described by NGO that, thanks to their hitherto unexploited nonlinearity, can make the output field modes *interfere constructively or destructively*, depending on the nonlinear couplings and the *mean quanta numbers* of the thermal input modes. In contrast, LIGO are incapable of performing this feat. The envisaged NGO can achieve both HE functionalities: heat concentration/steering from input modes to a designated output mode and partial heat-input conversion into ergotropy/work output in this mode.

From an information-theoretic perspective, such NGO cause information flow among the modes, resulting in *autonomous* feedforward of the information, as opposed to Maxwell-Demon based information engines [35–39] or externally-controlled HE [3–34]. The information flow and feedforward can change the thermal input states into *non-passive (ergotropy-carrying)* output states, while keeping the overall entropy constant (consistently with global coherence/unitarity).

When viewed quantum-mechanically, these NGO correlate the thermal input modes in ways inaccessible by LIGO, as quantified by the nonlinear unitary transformations of their mode-pair Stokes operators [60–62] and changes of their quantum statistical distributions. When viewed classically, the nonlinear couplings correlate the phases and amplitudes of different modes and thereby *stabilize* the interference against the random (thermal) phase and amplitude fluctuations. Namely, these nonlinear correlations permit to choose parameters that result in predominantly constructive interference of heat in a desired output mode, and destructive interference in undesired output modes. Significantly, *quantum correlations of the coupled modes incur vacuum noise that is a disadvantage for the functioning of HENLI compared to classical nonlinear correlations*.

To gain insight into the proposed general principle, we assume hot and cold baths that consist of a discrete set of  $N$  modes taken, for simplicity, to be at the same frequency (the consideration of non-degenerate modes is straightforward but laborious). These baths can be visualized as (ordered or disordered) *mode networks* that are divisible into repeated few-mode blocks: in each block, few output modes nonlinearly couple with similar numbers of thermal input modes, instead of (essentially infinite) mode continua in conventional baths. Each such block is a multiport nonlinear interferometer that is amenable to exact Hamiltonian analysis, both classically and quantum mechanically, without resorting to open-system approaches.

We discuss the HENLI principles from information-theoretic, classical and quantum mechanical perspectives, first generally and qualitatively (Sec. II) and then in detail for its minimal (4-mode) version (Sec. III) that can serve as a building block of such devices. Mutual information (MI) on phase-intensity intermode correlation, the feedforward of this information induced by nonlinear interference and the underlying quantum intermode correlations provide fundamentally new insights into this formidable problem. We then extend the analysis to a cascade of 4-mode HENLI blocks for scaled-up operation (Sec. IV).

Nonlinear networks for HENLI may be realized in various media, such as phononic structures [45] with anharmonically-coupled modes. Here (Sec. V) we discuss optomechanical setups with nonlinearly coupled photonic and phononic modes [63, 64], or photonic modes correlated by cross-Kerr polaritonic interaction [46–49, 65–69].

The new paradigm presented here, whereby heat machines can be purely coherent few-mode interferometers, lays the ground for bridging the conceptual gulf between nonlinear coherent dynamics and thermodynamics (Sec. VI).

## II. HENLI PRINCIPLES

To better understand the need for nonlinear NGO, consider first a linear interferometric network that transforms each input field mode into a linear combination of all others at the output [56, 57]. The output mode energies then depend on the phase differences of the input field modes. Yet, these phase differences are *unknown (random)* if the input is thermal. This randomness prevents selected-mode amplification or heat-to-work conversion [58, 59], because these functionalities are enabled by intermode mutual-information changes that are absent in coherent LIGO.

Concretely, consider a multiport interferometer with  $m$  input modes and  $m$  output modes that contains only (energy-conserving) linear mode couplers or beam splitters (BS). If a multimode factorized coherent state  $|\beta_1\rangle|\beta_2\rangle \dots |\beta_m\rangle$  is the input, one can find parameters of the interferometer that give rise to a coherent state  $|\alpha\rangle$

in output mode 1, all the remaining output modes being empty, i.e. full energy concentration is achievable. These LIGO are invertible, i.e. for a coherent state  $|\alpha\rangle$  at the input of mode 1 with the remaining  $m - 1$  input modes empty, the output modes will form a multimode factorized coherent state,  $|\beta_1\rangle|\beta_2\rangle \dots |\beta_m\rangle$ .

If, however, the input is thermal noise, it can be treated as a distribution of coherent states  $|\beta_1\rangle|\beta_2\rangle \dots |\beta_m\rangle$  with random amplitudes of  $\beta_1, \beta_2, \dots, \beta_m$  that have Gaussian distributions with zero mean. Neither of the HE functionalities are then achievable: (i) The multimode interference is washed out, prohibiting energy concentration. Notably, if the input modes have equal temperature (mean intensity), so will the output modes under LIGO. (ii) A passive (thermal state) in each input mode remains passive in the corresponding output mode, i.e. no work can be extracted from the output by single-mode unitaries, since LIGO cannot change the state passivity [14–16, 32–34].

Yet, if we could estimate the magnitudes and phases of  $\beta_1, \beta_2, \dots, \beta_m$ , and feedforward the results for each realization of the random input, we would be able to choose the interferometer parameters such that the energy is *mostly concentrated* in mode 1 via constructive interference and the output state in this mode is rendered *non-passive* via NGO. Here we show that it is possible to achieve these estimation and feedforward *autonomously* by nonlinear cross-couplers that correlate mode pairs via their intensity-dependent phase shifts.

Such autonomous intensity and phase estimation cannot be achieved if all the input modes are in the same thermal state: Part of the inputs have to be (desirably) empty or (at least) in a colder thermal state than the hot ones, and thus serve as the cold (few-mode) bath. Otherwise, the second law, which prohibits the operation of HE fed by a single-temperature source, would be violated.

The general  $m$ -mode protocol of HENLI consists of two major stages (see Fig. 1 (a)):

a) *Sampling*: A fraction of each hot input field mode is split off and mixed with a corresponding cold field mode by a LIGO which is described as field-quadrature rotation in  $m$ -mode space, realized in optics by imbalanced BS. The cold-mode states then become *weak copies* of the respective hot-mode states: perfect weak copies if the cold modes are empty, imperfect if they are not. These  $m/2$  copies are combined by LIGO rotations, optically realized by 50/50 BS for pairs of weak copies. These LIGO will be shown to “sample” the phase-difference distribution of the input-modes: the “sampling” results are stored (encoded) by the intensity mixing ratio of the weak-copy outputs.

b) *Nonlinear feedforward*: As we show, only if these weak-copy outputs are nonlinearly cross-correlated by NGO (here chosen to be nonlinear Kerr cross-coupling) with the set of the dominant (strong) hot-mode fractions, can the mixing ratio of the hot output modes at the final BS be controlled by the nonlinearity. These NGO can render the output distributions *non-thermal*. An addi-

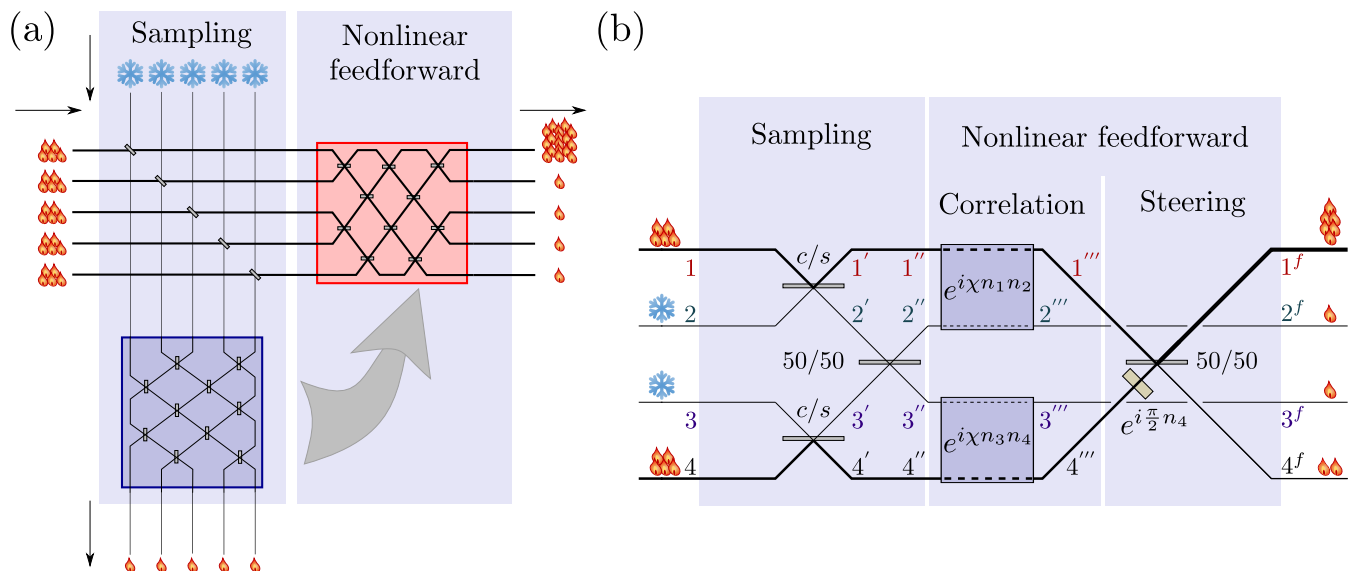


FIG. 1. (a) **A multiport nonlinear interferometer as a heat machine:** Input modes in a hot thermal state and those in a cold state undergo the following processes: (i) A fraction of the energy of the hot modes is split off by beam splitters. The split-off field (in the lower blue box) carries information about (“samples”) the field that remains in the hot modes. (ii) Nonlinear interactions correlate the two boxes. The information stored in the split-off field is converted via this correlation into autonomous feedforward (without the need to read and process the information) such that (iii) the thermal fields can be steered to interfere constructively in one preselected mode by parameter choice. (b) **A four-mode heat engine block based on a nonlinear-interferometer (HENLI)** in which the input modes (1 and 4—hot, 2 and 3—cold) undergo the stages described in the text. The parameters are chosen such that when averaged over all phases and amplitudes of the hot input modes and adding a linear  $\pi/2$  phase-shifter before the final BS, the interference is predominantly constructive in mode  $1^f$  and destructive in mode  $4^f$ .

tional LIGO ( $m$ -mode basis rotation and phase-shifting) exploits this nonlinear feedforward of the sampling to steer/concentrate the energy mainly to the desired mode.

These operations will be investigated in Sec. III for the minimal (4-mode) HENLI version. The analysis holds, however, for *any size of an interferometric network* which can be divided into 4-mode blocks (Sec. IV).

### III. MINIMAL HENLI ANALYSIS

Energy concentration must involve at least two hot modes, and each such mode is sampled (copied) by at least one cold mode (*the more copies the better*). Therefore, the minimal version of HENLI (shown in Fig. 1(b)) contains *two hot and two cold input modes at the same frequency*, labeled 1, 2, 3, and 4 from top to bottom. Extension to modes of different frequencies, to be presented elsewhere, does not reveal essentially new insights. Henceforth, we assume for simplicity that the cold input modes 2 and 3 are empty (an assumption that can be relaxed). Another assumption is that the coherence length of this 4-mode interferometer is much longer than its spatial size, so that temporal evolution can be replaced by *discrete steps* (stages), each described by a unitary evolution operator.

#### A. Phase-intensity distribution and information

We seek to control the energy transfer between the hot modes 1 and 4, and their output work capacity (ergotropy or non-passivity [14–16, 32–34]). To this end, we estimate and feedforward the a priori unknown amplitudes of the hot modes 1 and 4 so as to let them interfere, predominantly constructively in one port of the output BS and destructively in the other port. Instead of conventional measurements that can provide such information nearly perfectly [39], we settle here for partial, imperfect information that is autonomously extracted from cross-Kerr nonlinear coupling. It is extracted in the form of *mutual information (MI)* of the quantum-number difference  $n_-$  and phase difference  $\phi$  of between modes 1 and 4.

In each ( $k$ -th) stage of HENLI, their evolving correlations determine the MI, denoted by  $I_k$ , in terms of the joint distribution  $\mathcal{P}_k(n_-, \phi)$  and the marginal distributions  $p_k(n_-)$ ,  $\tilde{p}_k(\phi)$  [70]. The MI  $I_k$  usable for feedforward is given by [71]

$$I_k = \sum_{n_-} \int_0^{2\pi} \mathcal{P}_k(n_-, \phi) \ln \frac{\mathcal{P}_k(n_-, \phi)}{p_k(n_-)\tilde{p}_k(\phi)} d\phi. \quad (1)$$

Initially, the  $n_-$  and  $\phi$  distributions are uncorrelated,  $\mathcal{P}_0(n_-, \phi) = p_0(n_-)\tilde{p}_0(\phi)$ , where  $\tilde{p}_0(\phi) = 1/(2\pi)$  is the uniform distribution, so that their MI is zero. Total entropy conservation due to HENLI unitarity implies that

$I_k$  in Eq. (1) changes from one stage to another as a function of the entropies [6, 72]

$$I_k = \mathcal{S}_k(\{n_-\}) + \mathcal{S}_k(\phi) - [\mathcal{S}_{k-1}(\{n_-\}) + \mathcal{S}_{k-1}(\phi)], \quad (2)$$

$$\mathcal{S}_k(\{n_-\}) = \sum_{\{n_-\}} p_k(n_-) \ln[p_k(n_-)],$$

$$\mathcal{S}_k(\phi) = \int_{-\pi}^{\pi} d\phi \tilde{p}_k(\phi) \ln[\tilde{p}_k(\phi)].$$

This MI is evaluated for the consecutive stages of HENLI (Fig. 1(b), left to right):

(a) At the *sampling stage*, the first BS, with low transmissivity  $s = \sin \theta \ll 1$  (high reflectivity  $c = \cos \theta \lesssim 1$ ) cause small fractions of the hot input modes 1 and 4 to be split off and merge, respectively, with the empty modes 2 and 3. At the output of these BS, we then have weak copies 2' and 3' of each coherent-state amplitude in the random thermal distributions of modes 1 and 4, respectively. Namely, for each coherent-state realization, these weak copies have intensity difference that is proportional to  $n_-$  and the same phase-difference  $\phi$  as the input modes 1 and 4. The weak copies then merge on a 50/50 BS whose output modes 2'' and 3'' have amplitudes determined by the unknown  $-\pi \leq \phi \leq \pi$ . This is the “sampling” stage, since the initially uncorrelated distributions of  $n_-$  and  $\phi$  acquire correlations at the output of the 50/50 merger. When averaged over the thermal input ensembles (see SI), these correlations give rise to MI on the weak-copy modes (2-3) that encodes  $n_-$  via its dependence on  $\cos \phi$  at the output of 50/50 merger. This MI has the same form as Eq. (1). As a result, in the weak-copies the  $n_-$  distribution broadens (increases its entropy) while the  $\phi$  distribution is still uniform, as shown in Fig. 2a.

(b) At the *nonlinear feedforward stage*, two Kerr cross-couplers cause, in the classical approximation [73], the phase of the hot mode 1'' to be shifted proportionally to the intensity of mode 2'' and the phase of the hot mode 4'' to the mode 3'' intensity, so that  $\phi \rightarrow \phi + \chi n_-''$ . Thus, the cross-Kerr effect causes the coherent states with amplitudes  $|\alpha_1''\rangle$  and  $|\alpha_2'' \exp(i\phi)\rangle$  to become  $|\alpha_1'' \exp(i\chi \alpha_2''^2)\rangle$  and  $|\alpha_2'' \exp(i\phi + i\chi \alpha_1''^2)\rangle$ , respectively.

The exact quantum description of HENLI must account for the intermode entanglement of the field states that emerge from the sampling stage (see Sec. IIIB). For the MI analysis, however, it suffices to replace the exact intermode quantum correlations by their mean *in the classical approximation* which neglects quantum fluctuations and entanglement. For each set of coherent state amplitudes in the thermal input distribution,  $\{|\alpha_1\rangle, |0_2\rangle, |0_3\rangle, |\alpha_4 e^{i\phi}\rangle\}$ , we then have the following evolution stages:

(i) *Nonlinear correlation*: After the cross-Kerr couplers, the coherent-states in the strong-fraction hot modes 1''' and 4''' become, in this classical approximation,

$$|\alpha_1'''\rangle = |\alpha_1 \exp\left\{i\chi \frac{s^2}{2} |\alpha_1 + \alpha_4 e^{i\phi}|^2\right\}\rangle, \quad (3)$$

$$|\alpha_4'''\rangle = |\alpha_4 \exp\left\{i\left[\chi \frac{s^2}{2} |\alpha_1 - \alpha_4 e^{i\phi}|^2 + \phi\right]\right\}\rangle.$$

Thus, the phase shifts of the hot modes 1''' and 4''' that are merged by the second 50/50 BS are *nonlinearly correlated* and depend on  $\phi$  *non-sinusoidally*. We can infer the MI at the output from the  $(n_- - \phi)$  distribution of the modes 1''' and 4''' (Fig. 2b, SI). *The MI at the nonlinear correlation stage* ( $k = 2$  in Eq. 1) is *diminished* compared to that of the sampling stage ( $k = 1$ ), i.e.  $I_k$  is partly consumed to reduce  $\mathcal{S}_k(\phi)$  while  $\mathcal{S}_k(n_-)$  is unchanged. This means that the Kerr cross-coupling *feeds forward the information* encoded by  $\phi$ . The result of this nonlinear feedforward is a *sharply peaked (narrowed-down)*  $\phi$  distribution (Fig. 2c).

(ii) *Steering*: The final 50/50 BS, preceded by a  $\pi/2$  shift of mode 4''', yields at the two outputs the coherent-state amplitudes  $\alpha_{1,4}^f = 2^{-1/2}(\alpha_1'' \pm i\alpha_4''')$ , which determine the output intensities

$$|\alpha_{1,4}^f|^2 = \frac{c^2}{2} [\alpha_1^2 + \alpha_4^2 \pm 2\alpha_1\alpha_4 \sin(2s^2\alpha_1\alpha_4\chi \cos \phi - \phi)]. \quad (4)$$

This *non-sinusoidal* dependence of the interference term on the phase difference  $\phi$  of the input fields, stems from the nonlinearity of the feedforward. The final *narrow-peaked*  $\tilde{p}^f(\phi)$  allows, for appropriate  $\chi$  and  $s$ , to achieve predominantly destructive interference in mode 4<sup>f</sup> and constructive interference in mode 1<sup>f</sup> and thereby net transfer (steering) of mean intensity (energy) from mode 4 to mode 1 (or conversely), upon averaging over the random input amplitudes and phase differences  $\phi$  in the thermal input distribution,

$$\mathcal{P}(\alpha_1, \alpha_4, \phi) = \frac{2}{\pi \bar{n}^2} \alpha_1 \alpha_4 e^{-\frac{\alpha_1^2 + \alpha_4^2}{\bar{n}}} \quad (\text{Fig. 2d}).$$

We highlight the case of *equal input temperatures* which clearly shows that without cross-Kerr coupling there is no steering. The mean intensities at the output of the final 50/50 BS in the strong-fraction hot modes are, in this classical approximation,

$$\bar{n}_{1,4}^f = c^2 \bar{n} \left[ 1 \pm \frac{s^2 \chi \bar{n}}{(1 + s^4 \chi^2 \bar{n}^2)^2} \right]. \quad (5)$$

The optimal value of  $\chi$ ,  $\chi_{\text{opt}} = \frac{1}{\sqrt{3\bar{n}s^2}}$  when inserted in (5), yields  $(\bar{n}_1^f)_{(\text{max})} = c^2 \bar{n} \left(1 + \frac{9}{16\sqrt{3}}\right) \approx (4/3)c^2 \bar{n}$  (Fig. 3(b)). This result shows that the best strategy would be to split off as little of the incoming energy as possible ( $s^2 \ll 1$ ) and allow for large Kerr nonlinearity ( $\chi \gg 1$ ).

The steering ability due to nonlinear cross-coupling comes at a price: Part of the input energy leaks to the cold (initially empty) modes 2 and 3, so as to conserve sum of entropies of all modes, as required by the coherence of the process (SI).

## B. Intermode quantum correlations

(i) *Stokes operators*: The quantum correlations of the HENLI modes and their output nonthermal states that

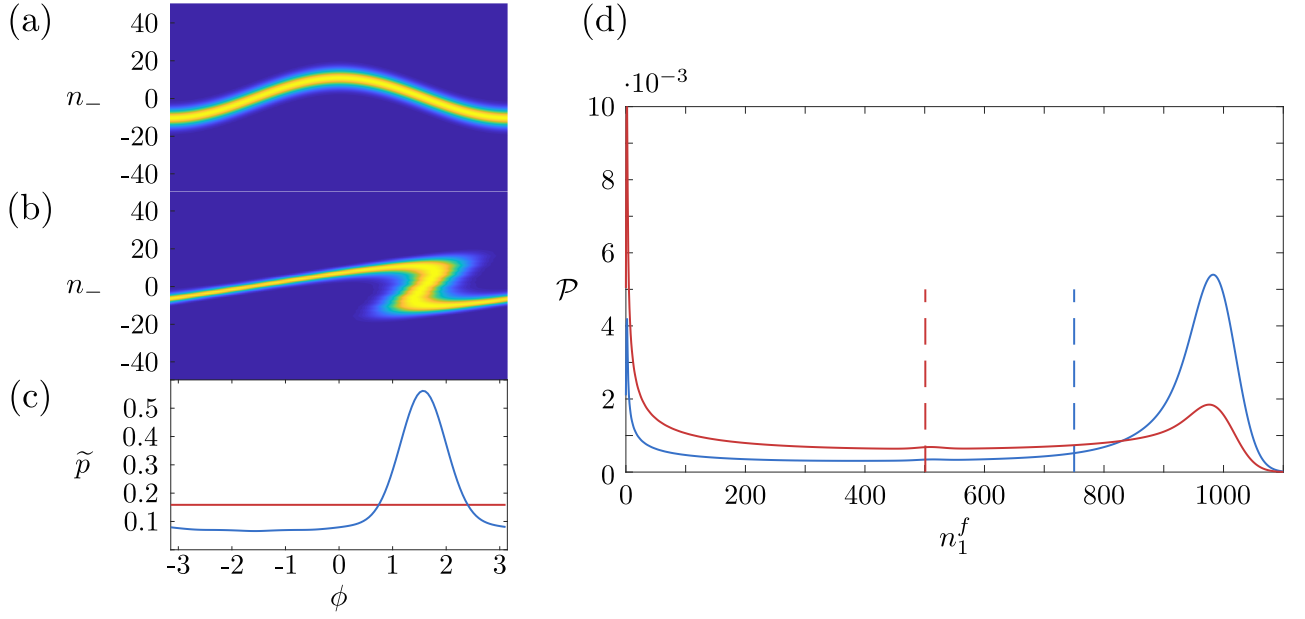


FIG. 2. (a) **Joint distribution**  $\mathcal{P}(n_-, \phi)$  of  $n_-$  and  $\phi$  after sampling stage. Brighter color denotes higher probability. (b) Same distribution after cross-Kerr stage. The change in  $n_- - \phi$  correlations yields a change in their mutual information. (c) Phase-difference distribution— initial (red) and final (blue). (d) Output quanta-number distribution in mode  $1^f$  for input thermal distribution. Red—no cross-Kerr, blue—with cross-Kerr, output with constructive interference (+ sign in Eq. (5)).

allow for steering of heat and work can be concisely captured by the two-mode Stokes operators [60–62, 74, 75]. The Stokes operators are expressed for modes  $i$  and  $j$  in terms of their annihilation operators  $\hat{a}_{i(j)}$

$$\begin{aligned}\hat{\mathcal{J}}_x^{(ij)} &= \frac{1}{2}(\hat{\mathcal{J}}_+^{(ij)} + \hat{\mathcal{J}}_-^{(ij)}), & \hat{\mathcal{J}}_y^{(ij)} &= \frac{-i}{2}(\hat{\mathcal{J}}_+^{(ij)} - \hat{\mathcal{J}}_-^{(ij)}), \\ \hat{\mathcal{J}}_+^{(ij)} &= \hat{a}_i^\dagger \hat{a}_j, & \hat{\mathcal{J}}_-^{(ij)} &= \hat{a}_i \hat{a}_j^\dagger, \\ \hat{\mathcal{J}}_z^{(ij)} &= \frac{1}{2}(\hat{a}_i^\dagger \hat{a}_i - \hat{a}_j^\dagger \hat{a}_j), & \hat{\mathcal{J}}_0^{(ij)} &= \frac{1}{2}(\hat{a}_i^\dagger \hat{a}_i + \hat{a}_j^\dagger \hat{a}_j).\end{aligned}\quad (6)$$

The fully quantum dynamics of the Stokes operators in HENLI is governed by the product of multimode unitary evolution operators that corresponds to the successive sampling (sa), cross-Kerr nonlinear (nl) and steering (st) stages described above. For the 4-mode version we have the unitary operator

$$\begin{aligned}\hat{U} &= \hat{U}_{\text{st}} \hat{U}_{\text{nl}} \hat{U}_{\text{sa}}, \\ \hat{U}_{\text{sa}} &= \hat{U}_{\text{bs}}^{(23)}(\pi/4) \hat{U}_{\text{bs}}^{(12)}(\theta) \hat{U}_{\text{bs}}^{(34)}(\theta), \\ \hat{U}_{\text{nl}} &= \hat{U}_{\text{cK}}^{(12)} \hat{U}_{\text{cK}}^{(34)}; & \hat{U}_{\text{cK}}^{(ij)} &= e^{i\chi \hat{n}_i \hat{n}_j}, \\ \hat{U}_{\text{st}} &= \hat{U}_{\text{bs}}^{(14)}(\pi/4) e^{-i\pi \hat{n}_4/2},\end{aligned}\quad (7)$$

where  $\hat{U}_{\text{bs}}^{(ij)}(\theta) = e^{2i\theta \hat{j}_y^{(ij)}}$  is a two-mode BS-mixing operator and  $\hat{U}_{\text{cK}}$  is the cross-Kerr operator. Both  $\hat{U}_{\text{sa}}$  and  $\hat{U}_{\text{st}}$  are LIGO rotations on the 4-mode Poincaré sphere, whereas  $\hat{U}_{\text{nl}}$  is a “twisting” NGO that entangles all modes in a nonlinear fashion.

The Stokes operators at the output ( $f$ ) are found to be related to their input ( $in$ ) counterparts in an exactly solvable, intricate nonlinear fashion (SI). The total population of the four modes is conserved according to the unitarity of the transformation Eq. (7), while the population difference operator of the hot output modes 1 and 4 is determined by the ( $\chi$ -dependent) exponential of combined  $\hat{\mathcal{J}}_x^{(ij)}$  operators of all four modes (SI). Whereas for  $\chi = 0$ , this is a trivial BS-induced LIGO, the population difference operator  $(\hat{\mathcal{J}}_z^{(14)})^{(f)}$  for  $\chi \neq 0$ , depends on the intermode correlations created at the sampling stage via the exponential factor  $e^{-2i\chi \hat{\mathcal{J}}_x^{(23)'}}$ , where  $\hat{\mathcal{J}}_x^{(23)'} = \left[ -s^2 \hat{\mathcal{J}}_x^{(14)} + c^2 \hat{\mathcal{J}}_x^{(23)} + sc(\hat{\mathcal{J}}_x^{(24)} - \hat{\mathcal{J}}_x^{(13)}) \right]^{(in)}$ . This quantum-nonlinear Kerr-induced NGO distorts (“twists”) and entangles the input inter-mode distribution.

(ii) *Stokes parameters* are the mean values of the Stokes operators. Here we are interested in the Stokes parameters of modes 1 and 4,

$$S_k = \langle \hat{\mathcal{J}}_k^{(14)} \rangle, \quad k = x, y, z, 0. \quad (8)$$

One can associate any two-mode coherent state with a point  $(S_x, S_y, S_z)$  on the surface of a Poincaré sphere of radius  $S_0$ . Under thermal-ensemble averaging, the first two BS are (“sampling”) LIGO that rotate the distribution, but the crucial nonlinear stage *concentrates* the random phase-space points on the surface of the hemisphere  $S_y < 0$  (Fig. 3a). The  $\pi/2$  phase shifter in mode  $4'''$  and the output BS correspond to a rotation around

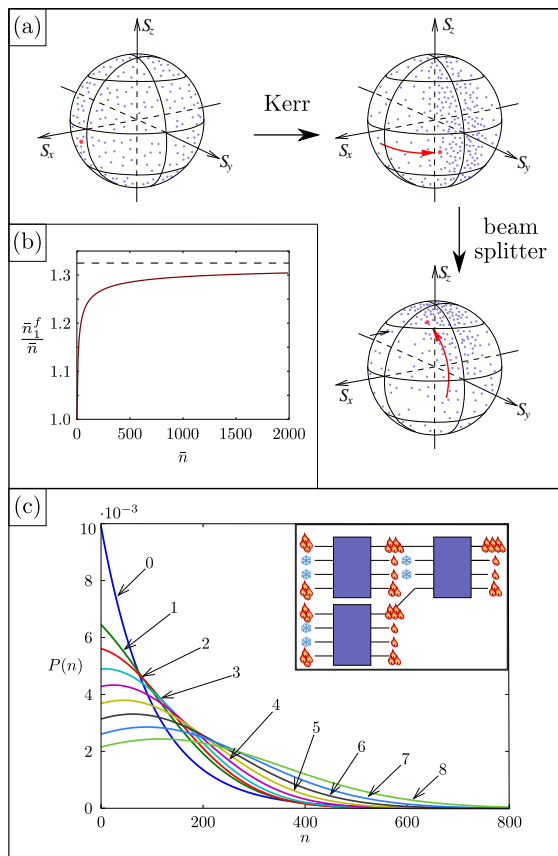


FIG. 3. (a) **Scheme of the transformations on the 2-mode Poincaré sphere of modes 1 and 4.** The cross-Kerr interaction concentrates the states in the negative  $S_y$  hemisphere and the final beam splitter rotates the sphere by  $\pi/2$  around  $S_x$  to move the states towards  $S_z > 0$ . Blue dots represent coherent states initially distributed randomly on the Poincaré sphere. The red point is a randomly chosen state for which the red arrows show the transformations. The distorted distribution is eventually concentrated near the north pole (maximal  $S_z$ ). (b) Mean output quanta number in mode  $1^f$ ,  $\bar{n}_1^f$ , normalized to the mean input quanta number  $\bar{n}$  plotted vs  $\bar{n}$  for thermal states of equal temperature in the hot modes 1 and 4 and optimized parameters  $\chi$  and  $s$ . Full line: fully quantum calculation, broken line: classical approximation (see SI). (c) **Inset: Cascading the HENLI blocks:** The highest-energy outputs of each block are used as the hot-mode inputs of the next one, thus gradually increasing the mean energy of a preselected mode.; **Quantum-number distribution** of the highest energy outputs in 8 consecutive blocks shows growing displacement of the distribution mean, corresponding to an increasing **work capacity (non-passivity)** of the output.

$S_x$  by  $\pi/2$ . This steering stage brings the phase-space points concentrated on the  $S_y < 0$  hemisphere surface to the  $S_z > 0$  hemisphere surface. Such *energy steering* does not violate the Liouville theorem, since the contraction of the phase-space volume occupied by modes 1 and 4 is compensated by the expansion of the volume corresponding to modes 2 and 3.

When the input modes 1 and 4 are quantum coherent states with equal amplitudes,  $\alpha_1 = \alpha_4$  and random phases, their Stokes parameters at the output, averaged over their random phase difference  $\phi$ , yield (SI)

$$\bar{S}_x^{(f)} = \bar{S}_y^{(f)} = 0, \quad \bar{S}_z^{(f)} = c^2 \alpha_1^2 e^{-d} J_1(b), \quad \bar{S}_0^{(f)} = c^2 \alpha_1^2, \quad (9)$$

where the overbar denotes the average over  $\phi$ ,  $d = s^2(1 - \cos \chi)(\alpha_1^2 + \alpha_4^2)$  and  $J_1(b)$  is the first order Bessel function with argument  $b = 2s^2 \alpha_1 \alpha_4 \sin \chi$ . The average quanta numbers of the output modes are found to be

$$\overline{\langle \hat{n}_{1,4}^{(f)} \rangle} = \bar{S}_0^{(f)} \pm \bar{S}_z^{(f)} = c^2 \alpha_1^2 [1 \pm J_1(b) e^{-d}], \quad (10)$$

where  $\hat{n}_i = \hat{a}_i^\dagger \hat{a}_i$ . When the fields in HENLI are classical, we obtain the average Stokes parameters and field intensities given by Eqs. (9) and (10) with  $d = 0$  and  $b = 2s^2 \alpha_1 \alpha_4 \chi$  (the quantum and classical expressions for  $b$  coincide when  $\chi \ll 1$ —see SI). A nonzero  $d$  results from quantum entanglement, created by the Kerr effect, and vacuum fluctuations of the modes. The exponential decay factor  $d$  thus diminishes the energy steering in Eqs. (9), (10) as compared to Eq. (5) in the classical approximation (Fig. 3b).

#### IV. QUANTUM DISTRIBUTION AND WORK PRODUCTION BY CASCADING

One can concentrate the energy to higher values than in Fig. 3b by cascading the 4-mode interferometric block described above (see inset in Fig. 3c). Such a cascade can be viewed as the *spatial analog of consecutive temporal cycles of a heat engine*. In each block, the relative variance  $\Delta n / \bar{n}$  is smaller than in the preceding one. As shown in Fig. 3c, this cascading yields as increasingly *non-monotonic quantum number distribution*  $\{p_n\} (n = 0, 1, 2, \dots)$  i.e. a growingly *non-passive state* with *net ergotropy* in the designated working mode, capable of delivering work [32–34] (see SI).

The interferometer parameters  $\chi$  and  $s$  have been optimized to maximize  $\bar{n} - \Delta n$  (i.e., the *non-passivity*) and not just  $\bar{n}$ . Although analytical formulae are tractable only for the first two moments of the quantum number distribution, we can put a bound on the *non-monotonicity* of the distribution. To this end, consistently with the Jaynes principle [76], we choose the quanta number distribution of the *highest entropy* that corresponds to the values of the first two moments.

Invariably, the sum of the *single-mode entropies* of the cascaded HENLI increases (but the total entropy remains constant). The input energy fraction converted to work is below the Carnot bound. The ability to attain this bound by cascading is yet to be studied, and so is the steady-state of such a cascade.

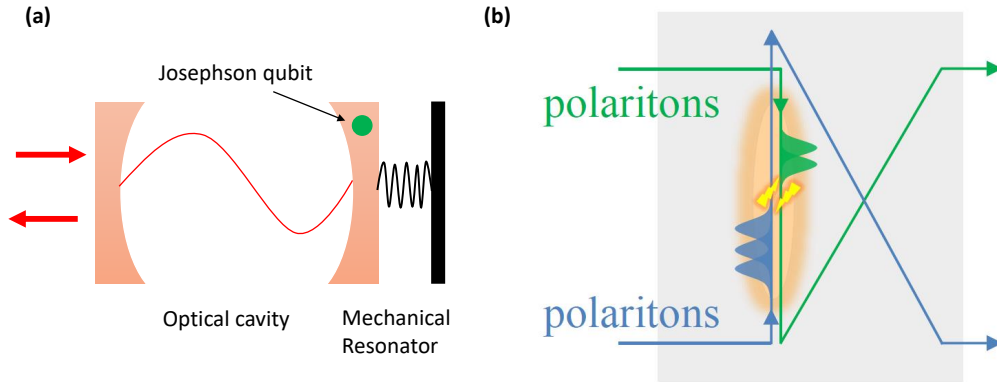


FIG. 4. (a) **Optomechanical implementation:** Optical cavity and mechanical resonator Kerr cross-coupled by a Josephson qubit [63]. (b) **Quantum nonlinear optical implementation:** Photons entering from the two input modes counter-propagate in the form of Rydberg slow-light polaritons. Giant dipole-dipole interaction between Rydberg atoms leads to a cross-Kerr phase shift of  $n_1 n_2 \pi / 2$  for counter-propagating  $n_1$  and  $n_2$  photons.

## V. ENVISAGED EXPERIMENTAL IMPLEMENTATIONS

(a) *Optomechanical setup:* The proposed scheme of HENLI can be implemented in an optomechanical setup where a microwave cavity is coupled to a mechanical resonator (Fig. 4a) with strength  $g$  [77]. The cross-Kerr coupling between the cavity and resonator can be induced by a Josephson junction qubit [63]. Due to this coupling, the cavity and mechanical resonator will have an effective cross-Kerr interaction Hamiltonian  $H_{cK} = \chi a^\dagger a b^\dagger b$ . As a result, the phase shift in the cavity field will depend on the number of phonons in the mechanical resonator. The estimated cross-Kerr strength for this optomechanical setup has been found to be very large,  $\chi = 0.25g$  [63].

(b) *Slow-light Rydberg polaritons:* Another feasible implementation may invoke a cross-Kerr nonlinear element using cold atomic vapor cells. The concept of such an element stems from our theoretical ideas [65, 66] and the experiments which demonstrated [67–69] *giant cross-Kerr nonlinearity* between few-photon beams converted into Rydberg polaritons (Fig. 4b). Their dipolar interaction (either dipole blockade [68] or resonant dipolar exchange [69]) can be tuned to yield a phase shift of  $\chi = \pi/2$  between each pair of counter-propagating polaritons.

## VI. CONCLUSIONS

Nonlinear interferometric networks have been proposed here for the first time as *fully coherent* heat engines (heat engines via nonlinear interferometry–HENLI). Conceptually, they allow us to *treat baths as dynamical systems*, in contrast to existing classical and quantum heat engine, for which the working-medium-bath exchange has *never been described as a coherent pro-*

*cess*. Such a description is indeed unfeasible for infinite/macrosopic baths, but here we consider only *few-mode “baths”*, distancing ourselves from the ruling paradigm of thermodynamics. Notwithstanding its coherent-nonlinear nature, HENLI adheres to the second law and acts as a genuine heat machine cycle, albeit only few modes are involved in the operation.

The minimal version of HENLI–4-mode cross-Kerr coupled network has been analyzed here to illustrate the operation principles. These nonlinearly-coupled modes replace both the working medium and the piston (working mode) so that HENLI is conceptually much simpler than a traditional heat engine. In principle, the analysis has revealed these general insights: (i) Mutual information of two-mode intensity-phase difference ( $n_- - \phi$ ) autonomously builds up by their sampling via a linear Gaussian operation and is then reduced via nonlinear correlation that narrows down the distribution  $\tilde{p}(\phi)$ . The final  $\tilde{p}(\phi)$  is part of the feedforward that controls the interference of output modes and thereby steers energy to the designated mode. (ii) The two-mode Stokes operators reveal quantum nonlinear 4-mode correlations that concentrate the population in a designated mode, and render its distribution non-thermal, but also incur performance-degrading due to admixing of vacuum noise through empty ports. (iii) Appropriate cascading of 4-mode HENLI blocks can progressively augment the energy steering to and the non-passivity of the designated mode, and its non-passivity analogously to consecutive cycles.

More sophisticated versions (to be reported) involve more modes (up to 8 modes) in each block, in order to obtain MI not only on ( $n_- - \phi$ ) distribution but also on other pairs of conjugate variables, thus rendering their sampling and feedforward more complete. Such a multimode block may realize functionalities other than HE (e.g. refrigerator [50] or heat transistor [52–54]).

On the applied side (a) HENLI devices may give rise

to new technologies of steering ambient heat (few-quanta input) in multimode networks and its conversion to quasi-coherent work output. Their practical value is their ability to *interfere and thereby concentrate energy from independent heat channels*. This feat is impossible in conventional heat devices, whose heat channels do not interfere. (b) The cascading process depicted here (Fig. 3c) may pave the way to *manipulating and enhancing the information hidden in noisy input via controllable nonlinear operations*. This perspective is based on the remarkable fact that HENLI bears analogy to a quantum computer with continuous variables [78], if inter-mode quantum correlations are accounted for, or to a semiclassical optical computer if they are neglected. (c) The feasibility of HENLI for few-photon or few-phonon input may add impetus to the creation of quantum nonlinear interference devices [65–69, 78].

By breaking away from the thermodynamic paradigm of dissipative HE operation, our long-term goal is to *trace the transition from quantum or classical coherent dynamics to thermodynamics* as a function of the number of bath modes and their nonlinear coupling.

Such a transition may provide the conceptual basis for a *unified thermodynamic coherent approach* whereby only the input channels are thermal while the rest of the process is classically or quantum-mechanically coherent.

**Acknowledgments** T.O. and Š.B. are supported by the Czech Science Foundation, Grant No. 20- 27994S. Š.B. is supported by project IGA-PrF-2022-005. G.K. is supported by ISF, DFG (FOR 2724) and QUANTERA (PACE-IN). E.P., O.F. and G.K. are supported by NSF-BSF.

**Author contributions:** All the authors contributed to the formulation of the problem, its analysis and the discussion of its results. TO, AGK, AM and NM have carried out the analytical calculations, whereas SB has performed the numerical work. EP, OF, TO and NM have analyzed the possible experimental implementations. GK, TO and AGK have done most of the writing.

**Competing interests:** The authors declare no competing interests.

- 
- [1] H. B. Callen, *Thermodynamics and an Introduction to Thermostatistics* (John Wiley & Sons, Inc., 1985).
- [2] D. Kondepudi and I. Prigogine, *Modern Thermodynamics: From Heat Engines to Dissipative Structures, 2nd edition* (Wiley, Chichester, 2014).
- [3] R. Kosloff, Quantum thermodynamics: A dynamical viewpoint, *Entropy* **15**, 2100 (2013).
- [4] F. Binder, L. Correa, C. Gogolin, J. Anders, and G. e. Adesso, *Thermodynamics in the Quantum Regime: Fundamental Aspects and New Directions* (Springer, 2018).
- [5] D. Gelbwaser-Klimovsky, W. Niedenzu, and G. Kurizki, Chapter twelve - thermodynamics of quantum systems under dynamical control (Academic Press, 2015) pp. 329–407.
- [6] G. Kurizki and A. G. Kofman, *Thermodynamics and Control of Open Quantum Systems* (Cambridge University Press, 2022).
- [7] H. E. D. Scovil and E. O. Schulz-DuBois, Three-level masers as heat engines, *Phys. Rev. Lett.* **2**, 262 (1959).
- [8] R. Alicki, The quantum open system as a model of the heat engine, *Journal of Physics A: Mathematical and General* **12**, L103 (1979).
- [9] X. L. Huang, T. Wang, and X. X. Yi, Effects of reservoir squeezing on quantum systems and work extraction, *Phys. Rev. E* **86**, 051105 (2012).
- [10] M. O. Scully, M. S. Zubairy, G. S. Agarwal, and H. Walther, Extracting work from a single heat bath via vanishing quantum coherence, *Science* **299**, 862 (2003).
- [11] R. Uzdin, A. Levy, and R. Kosloff, Equivalence of quantum heat machines, and quantum-thermodynamic signatures, *Phys. Rev. X* **5**, 031044 (2015).
- [12] M. Campisi and R. Fazio, The power of a critical heat engine, *Nature Communications* **7**, 11895 (2016).
- [13] J. Roßnagel, S. T. Dawkins, K. N. Tolazzi, O. Abah, E. Lutz, F. Schmidt-Kaler, and K. Singer, A single-atom heat engine, *Science* **352**, 325 (2016), [arXiv:1510.03681](https://arxiv.org/abs/1510.03681) [[cond-mat.stat-mech](https://arxiv.org/abs/1510.03681)].
- [14] D. Gelbwaser-Klimovsky, R. Alicki, and G. Kurizki, Work and energy gain of heat-pumped quantized amplifiers, *EPL* **103**, 60005 (2013).
- [15] D. Gelbwaser-Klimovsky and G. Kurizki, Heat-machine control by quantum-state preparation: From quantum engines to refrigerators, *Phys. Rev. E* **90**, 022102 (2014).
- [16] W. Niedenzu, D. Gelbwaser-Klimovsky, A. G. Kofman, and G. Kurizki, On the operation of machines powered by quantum non-thermal baths, *New Journal of Physics* **18**, 083012 (2016).
- [17] C. B. Dağ, W. Niedenzu, O. E. Müstecaplıoğlu, and G. Kurizki, Multiatom quantum coherences in micro-masers as fuel for thermal and nonthermal machines, *Entropy* **18**, 10.3390/e18070244 (2016).
- [18] V. Mukherjee, W. Niedenzu, A. G. Kofman, and G. Kurizki, Speed and efficiency limits of multilevel incoherent heat engines, *Phys. Rev. E* **94**, 062109 (2016).
- [19] A. Ghosh, C. L. Latune, L. Davidovich, and G. Kurizki, Catalysis of heat-to-work conversion in quantum machines, *Proceedings of the National Academy of Sciences* **114**, 12156 (2017).
- [20] A. Ghosh, D. Gelbwaser-Klimovsky, W. Niedenzu, A. I. Lvovsky, I. Mazets, M. O. Scully, and G. Kurizki, Two-level masers as heat-to-work converters, *Proceedings of the National Academy of Sciences* **115**, 9941 (2018).
- [21] W. Niedenzu, V. Mukherjee, A. Ghosh, A. G. Kofman, and G. Kurizki, Quantum engine efficiency bound beyond the second law of thermodynamics, *Nature Communications* **9**, 165 (2018).
- [22] R. Dillenschneider and E. Lutz, Energetics of quantum correlations, *EPL (Europhysics Letters)* **88**, 50003

- (2009).
- [23] O. Abah and E. Lutz, Efficiency of heat engines coupled to nonequilibrium reservoirs, *EPL (Europhysics Letters)* **106**, 20001 (2014).
- [24] J. Roßnagel, O. Abah, F. Schmidt-Kaler, K. Singer, and E. Lutz, Nanoscale heat engine beyond the carnot limit, *Phys. Rev. Lett.* **112**, 030602 (2014).
- [25] A. . C. Hardal and z. E. Müstecaplıođlu, Superradiant quantum heat engine, *Scientific Reports* **5**, 12953 (2015).
- [26] J. Klaers, S. Faelt, A. Imamoglu, and E. Togan, Squeezed thermal reservoirs as a resource for a nanomechanical engine beyond the carnot limit, *Phys. Rev. X* **7**, 031044 (2017).
- [27] C. Mukhopadhyay, A. Misra, S. Bhattacharya, and A. K. Pati, Quantum speed limit constraints on a nanoscale autonomous refrigerator, *Phys. Rev. E* **97**, 062116 (2018).
- [28] A. Misra, U. Singh, M. N. Bera, and A. K. Rajagopal, Quantum rényi relative entropies affirm universality of thermodynamics, *Phys. Rev. E* **92**, 042161 (2015).
- [29] S. Das, A. Misra, A. K. Pal, A. Sen(De), and U. Sen, Necessarily transient quantum refrigerator, *Euro Phys. Lett.* **125**, 20007 (2019).
- [30] M. T. Mitchison, M. P. Woods, J. Prior, and M. Huber, Coherence-assisted single-shot cooling by quantum absorption refrigerators, *New Journal of Physics* **17**, 115013 (2015).
- [31] B. Gardas and S. Deffner, Thermodynamic universality of quantum carnot engines, *Phys. Rev. E* **92**, 042126 (2015).
- [32] A. E. Allahverdyan, R. Balian, and T. M. Nieuwenhuizen, Maximal work extraction from finite quantum systems, *Europhysics Letters (EPL)* **67**, 565 (2004).
- [33] W. Pusz and S. L. Woronowicz, Passive states and kms states for general quantum systems, *Comm. Math. Phys.* **58**, 273 (1978).
- [34] A. Lenard, Thermodynamical proof of the gibbs formula for elementary quantum systems, *Journal of Statistical Physics* **19**, 575 (1978).
- [35] E. Lutz and S. Ciliberto, Information: From Maxwell’s demon to Landauer’s eraser, *Phys. Today* **68**, 30 (2015).
- [36] M. D. Vidrighin, O. Dahlsten, M. Barbieri, M. S. Kim, V. Vedral, and I. A. Walmsley, Photonic Maxwell’s demon, *Phys. Rev. Lett.* **116**, 050401 (2016).
- [37] Z. Lu and C. Jarzynski, A programmable mechanical maxwell’s demon, *Entropy* **21**, 10.3390/e21010065 (2019).
- [38] H. S. Leff and A. F. Rex, *Maxwell’s Demon: Entropy, Information, Computing* (Princeton University Press, 2014).
- [39] T. Opatrny, A. Misra, and G. Kurizki, Work generation from thermal noise by quantum phase-sensitive observation, *Phys. Rev. Lett.* **127**, 040602 (2021).
- [40] E. G. Brown, N. Friis, and M. Huber, Passivity and practical work extraction using gaussian operations, *New Journal of Physics* **18**, 113028 (2016).
- [41] U. Singh, M. G. Jabbour, Z. Van Herstraeten, and N. J. Cerf, Quantum thermodynamics in a multipartite setting: A resource theory of local gaussian work extraction for multimode bosonic systems, *Phys. Rev. A* **100**, 042104 (2019).
- [42] A. Serafini, M. Lostaglio, S. Longden, U. Shackerley-Bennett, C.-Y. Hsieh, and G. Adesso, Gaussian thermal operations and the limits of algorithmic cooling, *Phys. Rev. Lett.* **124**, 010602 (2020).
- [43] V. Narasimhachar, S. Assad, F. C. Binder, J. Thompson, B. Yadin, and M. Gu, Thermodynamic resources in continuous-variable quantum systems, *npj Quantum Information* **7**, 10.1038/s41534-020-00342-6 (2021).
- [44] B. Yadin, H. H. Jee, C. Sparaciari, G. Adesso, and A. Serafini, Catalytic gaussian thermal operations (2021), [arXiv:2112.05540 \[quant-ph\]](https://arxiv.org/abs/2112.05540).
- [45] S. Ding, G. Maslennikov, R. Hablützel, and D. Matsukevich, Cross-kerr nonlinearity for phonon counting, *Phys. Rev. Lett.* **119**, 193602 (2017).
- [46] G. J. Milburn and D. F. Walls, Quantum nondemolition measurements via quadratic coupling, *Phys. Rev. A* **28**, 2065 (1983).
- [47] N. Imoto, H. A. Haus, and Y. Yamamoto, Quantum nondemolition measurement of the photon number via the optical kerr effect, *Phys. Rev. A* **32**, 2287 (1985).
- [48] J. C. Howell and J. A. Yeazell, Nondestructive single-photon trigger, *Phys. Rev. A* **62**, 032311 (2000).
- [49] W. J. Munro, K. Nemoto, R. G. Beausoleil, and T. P. Spiller, High-efficiency quantum-nondemolition single-photon-number-resolving detector, *Phys. Rev. A* **71**, 033819 (2005).
- [50] M. Kolář, D. Gelbwaser-Klimovsky, R. Alicki, and G. Kurizki, Quantum bath refrigeration towards absolute zero: Challenging the unattainability principle, *Phys. Rev. Lett.* **109**, 090601 (2012).
- [51] D. Gelbwaser-Klimovsky, R. Alicki, and G. Kurizki, Minimal universal quantum heat machine, *Phys. Rev. E* **87**, 012140 (2013).
- [52] B. Karimi, J. P. Pekola, M. Campisi, and R. Fazio, Coupled qubits as a quantum heat switch, *Quantum Science and Technology* **2**, 044007 (2017).
- [53] M. T. Naseem, A. Misra, O. E. Müstecaplıođlu, and G. Kurizki, Minimal quantum heat manager boosted by bath spectral filtering, *Phys. Rev. Research* **2**, 033285 (2020).
- [54] C. Karg ı, M. T. Naseem, T. c. v. Opatrny, O. E. Müstecaplıođlu, and G. Kurizki, Quantum optical two-atom thermal diode, *Phys. Rev. E* **99**, 042121 (2019).
- [55] J. Klatzow, J. N. Becker, P. M. Ledingham, C. Weinzetl, K. T. Kaczmarek, D. J. Saunders, J. Nunn, I. A. Walmsley, R. Uzdin, and E. Poem, Experimental demonstration of quantum effects in the operation of microscopic heat engines, *Phys. Rev. Lett.* **122**, 110601 (2019).
- [56] M. Reck, A. Zeilinger, H. J. Bernstein, and P. Bertani, Experimental realization of any discrete unitary operator, *Phys. Rev. Lett.* **73**, 58 (1994).
- [57] W. R. Clements, P. C. Humphreys, B. J. Metcalf, W. S. Kolthammer, and I. A. Walmsley, Optimal design for universal multiport interferometers, *Optica* **3**, 1460 (2016).
- [58] E. A. Martinez and J. P. Paz, Dynamics and thermodynamics of linear quantum open systems, *Phys. Rev. Lett.* **110**, 130406 (2013).
- [59] N. Freitas and J. P. Paz, Analytic solution for heat flow through a general harmonic network, *Phys. Rev. E* **90**, 042128 (2014).
- [60] J. Schwinger, *Quantum Theory of Angular Momentum: A Collection of Reprints and Original Papers*, edited by H. V. D. L.C. Biedenharn (Academic Press, 1965).
- [61] G. S. Agarwal, *Quantum statistical theories of spontaneous emission and their relation to other approaches* (Springer-Verlag, Berlin Heidelberg, 1974).
- [62] U. Leonhardt, *Measuring the Quantum State of Light* (Cambridge Studies in Modern Optics, Cambridge,

- 1997).
- [63] T. T. Heikkilä, F. Massel, J. Tuorila, R. Khan, and M. A. Sillanpää, Enhancing optomechanical coupling via the Josephson effect, *Phys. Rev. Lett.* **112**, 203603 (2014).
- [64] G. Kurizki, P. Bertet, Y. Kubo, K. Mølmer, D. Petrosyan, P. Rabl, and J. Schmiedmayer, Quantum technologies with hybrid systems, *Proceedings of the National Academy of Sciences* **112**, 3866 (2015), <https://www.pnas.org/doi/pdf/10.1073/pnas.1419326112>.
- [65] E. Shahmoon, G. Kurizki, M. Fleischhauer, and D. Petrosyan, Strongly interacting photons in hollow-core waveguides, *Phys. Rev. A* **83**, 033806 (2011).
- [66] I. Friedler, D. Petrosyan, M. Fleischhauer, and G. Kurizki, Long-range interactions and entanglement of slow single-photon pulses, *Phys. Rev. A* **72**, 043803 (2005).
- [67] O. Firstenberg, T. Peyronel, Q.-Y. Liang, A. V. Gorshkov, M. D. Lukin, and V. Vuletić, Attractive photons in a quantum nonlinear medium, *Nature* **502**, 71 (2013).
- [68] J. D. Thompson, T. L. Nicholson, Q.-Y. Liang, S. H. Cantu, A. V. Venkatramani, S. Choi, I. A. Fedorov, D. Viscor, T. Pohl, M. D. Lukin, and V. Vuletić, Symmetry-protected collisions between strongly interacting photons, *Nature* **542**, 206 (2017).
- [69] D. Tiarks, S. Schmidt-Eberle, T. Stolz, G. Rempe, and S. Dürr, A photon–photon quantum gate based on Rydberg interactions, *Nature Physics* **15**, 124 (2019).
- [70] J. M. R. Parrondo, J. M. Horowitz, and T. Sagawa, Thermodynamics of information, *Nat. Phys.* **11**, 131 (2015).
- [71] T. M. Cover, *Elements of information theory* (New York : Wiley, 1991).
- [72] A. Misra, T. Opatrny, and G. Kurizki, Work extraction from single-mode thermal noise by measurements: How important is information?, arXiv [10.48550/ARXIV.2201.11567](https://arxiv.org/abs/10.48550/ARXIV.2201.11567) (2022).
- [73] R. W. Boyd, *Nonlinear Optics* (Academic Press, Burlington, 2008).
- [74] J. M. Jauch and F. Rohrlich, *The Theory of Photons and Electrons* (Springer, 1976).
- [75] B. A. Robson, *The Theory of Polarization Phenomena* (Oxford, 1974).
- [76] E. T. Jaynes, Information theory and statistical mechanics, *Phys. Rev.* **106**, 620 (1957).
- [77] M. Aspelmeyer, T. J. Kippenberg, and F. Marquardt, Cavity optomechanics, *Rev. Mod. Phys.* **86**, 1391 (2014).
- [78] S. Lloyd and S. L. Braunstein, Quantum computation over continuous variables, *Phys. Rev. Lett.* **82**, 1784 (1999).